Thin Solid Films 558 (2014) 184–188

Contents lists available at ScienceDirect

Thin Solid Films

journal homepage: www.elsevier.com/locate/tsf

Growth of polycrystalline Ag/Ni multilayers at room temperature

Y. Muhammad [a,b], F. Magnus [a,*], T. Thersleff [c], P. Poulopoulos [d], V. Kapaklis [a], K. Leifer [c], B. Hjörvarsson [a]

[a] *Department of Physics and Astronomy, Uppsala University, Box 516, SE-751 20 Uppsala, Sweden*
[b] *Department of Physics, Government College University Lahore, Lahore 54000, Pakistan*
[c] *Department of Engineering Sciences, Division of Applied Materials Science, Uppsala University, Box 534, SE-751 21 Uppsala, Sweden*
[d] *Department of Materials Science, School of Natural Sciences, University of Patras, GR-26504 Patras, Greece*

ARTICLE INFO

Article history:
Received 20 December 2013
Received in revised form 5 March 2014
Accepted 14 March 2014
Available online 21 March 2014

Keywords:
Multilayers
Room temperature deposition
Amorphous
Interlayer exchange coupling

ABSTRACT

Ag/Ni multilayers have been grown on oxidized Si(100) substrates by dc magnetron sputtering at room temperature. The Ag thickness is varied in the range 2.5–20 Å. A combination of X-ray reflectivity, diffraction and transmission electron microscopy shows that the films have excellent layering for all Ag thicknesses. This is due to the use of an amorphous AlZr wetting layer which promotes smooth, layered growth of the Ag and Ni. The results demonstrate the feasibility of growing good quality multilayers of high mobility metals on oxide substrates without substrate cooling.

1. Introduction

Multilayered materials have received considerable interest in recent years, mainly due to their technological applications in giant magnetoresistance (GMR) sensors [1] and perpendicular magnetic recording media [2]. However, multilayers (the non-coherent counterpart of superlattices) have a wider appeal as they provide us with a means to study the influence of reduced thickness, interfaces and interlayer coupling on a variety of physical properties. In the case of magnetism, reduced dimensionality can have profound effects on the magnetic ordering [3], and interfaces can result in spin-dependent scattering [4,5] as well as having different anisotropy from the "bulk" material [6,7]. Furthermore, interlayer coupling can give rise to effects such as proximity induced magnetism [8], interlayer exchange coupling [9] and dipolar coupling in patterned structures [10].

Ag/Ni multilayers have been studied intensively due to their potential for high GMR ratios [11–13]. Recently however, the possibility of coupling the magnetic properties of ferromagnets with the plasmonic properties of the noble metals has been recognized, giving rise to the field of magnetoplasmonics [14]. As an example, surface plasmons have been found to enhance strongly the magneto-optical response of Au coated Ni anti-dot arrays [15]. Ag and Ni are immiscible metals and therefore they should produce sharp interfaces [11]. However, silver-containing multilayers are particularly challenging to manufacture due to the high mobility of silver on substrates such as SiO_2 resulting in extreme Volmer–Weber (or island) growth [16] which is strongly detrimental to the layering quality. Therefore, liquid nitrogen temperatures were previously needed to obtain satisfactory layering in Ag/Ni multilayers [11,13,17,18], which is highly undesirable from a practical point of view.

Here, we demonstrate a route to obtain high quality Ag/Ni multilayers with room temperature magnetron sputtering. This is achieved through the use of an amorphous AlZr seeding layer which has been shown to grow amorphous (and therefore atomically flat) on Si substrates [19,20]. The AlZr ensures wetting of the substrate by subsequent layers, thus reducing roughness and promoting well-layered growth [21]. We examine the layering quality by X-ray scattering and electron microscopy and we also study how the magnetic properties vary with the non-magnetic interlayer thickness.

2. Experiment

The Ag/Ni multilayers were grown in an ultrahigh vacuum system by dc magnetron sputtering. The base pressure of the system was better than 3×10^{-7} Pa and the pressure of the Ar gas during growth (with a purity of 99.9999%) was 0.27 Pa. All the samples were grown on Si(100) single-crystal substrates with the native oxide intact. The growth was carried out at room temperature but the substrates were annealed at 550 °C for 30 min prior to deposition to remove surface impurities. The substrates were rotated during deposition to get a uniform thickness. First, a 20 Å thick buffer layer of $Al_{0.7}Zr_{0.3}$ was deposited on the substrate from an AlZr alloy target to allow the growth of well defined layers of Ag. The AlZr has been shown to grow amorphous on Si substrates and facilitate the stabilization of amorphous phases in various alloys such as SmCo [21], FeZr [20] and CoFeZr [22]. Next, Ag and Ni layers

---

[*] Corresponding author.
E-mail address: fridrik.magnus@physics.uu.se (F. Magnus).

http://dx.doi.org/10.1016/j.tsf.2014.03.052
0040-6090/

were alternately deposited from targets of 99.99% purity, with deposition rates of 1.21 Å/s and 1.05 Å/s, respectively, as calibrated using X-ray reflectivity measurements. The Ag/Ni bilayer was repeated 15 times and the first layer was Ag in all cases. To prevent oxidation of the Ag and the Ni layer, the samples were capped with a 30 Å $Al_{0.7}Zr_{0.3}$ layer. The layering of the sample is illustrated in the inset of Fig. 1. In all samples the thickness of the Ni layer was kept constant at 25 Å whereas the thickness of the Ag layer was varied between 2.5 and 20 Å.

Structural analysis was performed by X-ray diffraction (XRD), X-ray reflectivity (XRR) and cross-sectional transmission electron microscopy (TEM). The XRD was carried out using Cu Kα radiation with $\lambda = 1.5418$ Å in a Bragg–Brentano geometry with a monochromator on the diffracted side whereas the XRR was performed in a parallel beam geometry, using Cu $K\alpha_1$ radiation with $\lambda = 1.5406$ Å, selected by a Göbel mirror and a beam compressor yielding a wavelength spread of $\Delta\lambda / \lambda = 1 \times 10^{-4}$. Thicknesses of the layers, their densities and interface widths were determined by simulating the XRR data. A TEM lamella cross-section was prepared from the Ag/Ni 20/25 Å film. The lamella was prepared using the Focused Ion Beam (FIB) in-situ lift-out method on a Strata DB235 FIB from FEI company using an acceleration voltage of 30 kV. The sample was thinned to approximately 100 nm at this energy and then subsequently polished using gallium ions accelerated at 5 kV. The finished lamella had a thickness ranging from 45 to 65 nm in the measured region, as determined by Kramers–Krönig analysis. The sample was investigated in a Tecnai F30 TEM (FEI company) equipped with a SuperTwin objective lens operated at 300 kV and a Tridiem Gatan Image Filter.

Magnetic characterization of the samples was performed by magneto-optic Kerr effect (MOKE) measurements in the longitudinal geometry with s-polarized light. The samples were rotated around the azimuthal angle ϕ i.e. around the film normal and the full hysteresis loops were recorded at $\phi = 0°$, 45° and 90°. All measurements were performed at room temperature.

3. Results and discussion

The layering is clearly visible from XRR data, which shows first and second order Bragg peaks corresponding to the Ag/Ni multilayer period in all the samples. Some representative XRR scans are shown in Fig. 1. As the thickness of the Ag layer increases, so does the thickness of the bilayer which results in a shift of the Bragg peaks towards smaller 2θ values [23,24]. The height of the Bragg peaks increases with increasing Ag thickness due to the increased electron density contrast between the layers. The Bragg peak width also increases which is an indication of a smearing of the bilayer thickness, as a result of the increase in roughness with increasing total thickness. Also visible are the narrow Kiessig fringes with a periodicity corresponding to the total thickness of the film as well as wide fringes corresponding to the capping layer thickness. The data can be fitted by assuming the layer model depicted in the inset to Fig. 1 and such fits confirm that the bilayer thicknesses are within 5% of the designed thickness. In order to reproduce the anomalous width of the Bragg peaks, a linear increase of the interface roughness throughout the multilayer is assumed in the modeling. The simulated roughness corresponds to both thickness variation and waviness, which will be addressed below. The root-mean-squared roughness of the top layers is only approximately 15 Å for the 20/25 Å sample.

Fig. 2 shows transverse scans (rocking-curves) around the first order Bragg peak. In these scans, the out-of-plane scattering vector length is fixed at the 2θ value of a Bragg peak while the incident angle omega is varied. The high and narrow intensity profile around $\Delta\omega = 0$ corresponds to specular reflection whereas the broad background at higher Δω corresponds to diffuse scattering. For the thinnest Ag layer, only a specular scattering contribution is observed indicating a very low roughness but with increasing Ag thickness the specular peak is superimposed on a wide diffuse scattering background. Such diffuse scattering arises from thickness variation and waviness of the bilayers (simulated as interface roughness) which clearly increases with increasing Ag thickness. To quantify this we plot the ratio of the specular peak area to the total scattering area in the inset of Fig. 2. Despite the increase in diffuse scattering, the fraction of specular scattering increases with increasing Ag thickness. This shows that the layering is robust even in the thickest samples where roughening is producing a significant diffuse scattering contribution.

Both Ag and Ni grow with a [111] out-of-plane texture (the [111] direction is perpendicular to the film plane) on substrates where no epitaxial relationship with the Ag or Ni exists, such as amorphous SiO_2. The texture evolution of the Ag/Ni multilayers with increasing Ag thickness is presented in Fig. 3. Although a single layer of Ni has a clear [111]

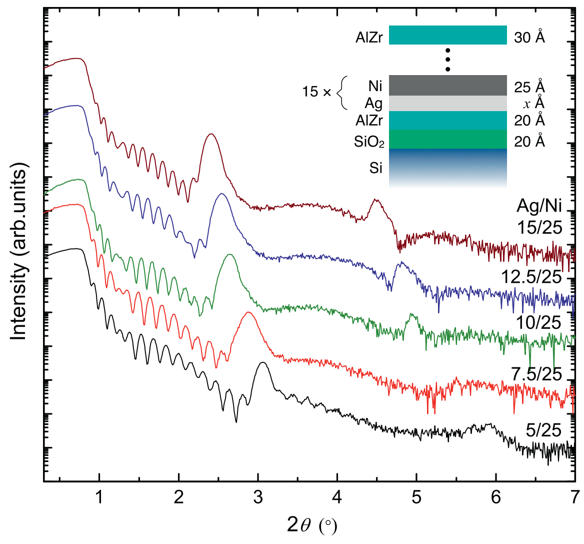

Fig. 1. X-ray reflectivity scans for samples with varied Ag layer thickness as indicated in Å. The scans are offset for clarity. First and second order multilayer peaks are clearly seen. Inset: The layer structure used for fitting the reflectivity.

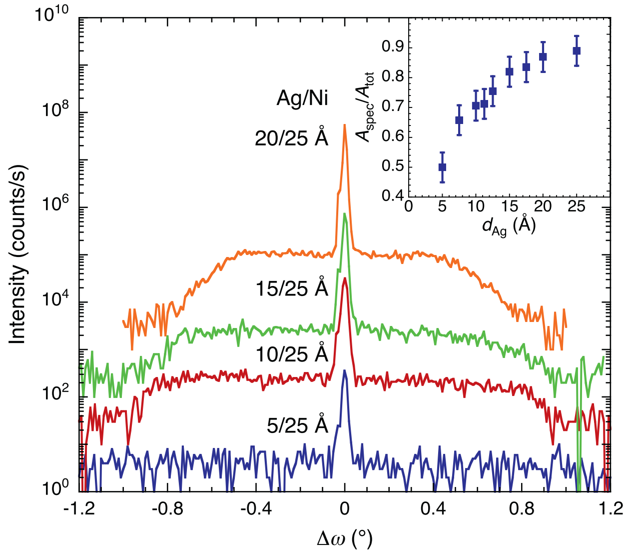

Fig. 2. Transverse scans (rocking-curves) around the first order bilayer peaks of the Ag/Ni multilayers. The specular peak is shifted to zero ω. The 10/25, 15/25 and 20/25 Å sample scans are shifted up by a factor of 10, 100 and 1000, respectively. Inset: The ratio of the area of the specular peak A_{spec} and the total area of the scattered X-rays A_{tot} (specular and non-specular), as a function of the Ag layer thickness. An increase in the A_{spec}/A_{tot} ratio is clearly seen with increasing thickness of non-magnetic spacer layer.